第 24 卷第 10 期 无 机 化 学 学 报 Vol.24 No.10
2008 年 10 月 CHINESE JOURNAL OF INORGANIC CHEMISTRY 1570~1575

钛酸钠纳米带的合成、表征与气敏性能

陶友荣 张玉玲 温乐乐 吴兴才*
(南京大学化学化工学院介观化学教育部重点实验室,南京 210093)

摘要:通过钛酸丁酯与氢氧化钠浓溶液的两步水热反应合成出宽度为 20~240 nm、厚度为 10~40 nm、长度达几十微米的单一物相的 $Na_2Ti_3O_7$ 纳米带。用 X-射线衍射和电子显微镜分别表征了它们的结构和形貌。这些纳米带被加工成化学电阻型传感器以测量气敏特性。测试表明在 350~400 ℃之间对丙酮、乙醇和二硫化碳具有明显感应,而对一氧化碳、苯、氨气和 30%的甲醛水溶液几乎不敏感。用化学吸附模型解释其气敏机理。

关键词:水热合成;钛;氧化物;纳米带;气敏传感器
中图分类号:O614.112; O614.41+1; TP212.2 **文献标识码**:A **文章编号**:1001-4861(2008)10-1570-06

Synthesis, Characterization and Gas-sensing Properties of Sodium Titanate Nanobelts

TAO You-Rong ZHANG Yu-Ling WEN Le-Le WU Xing-Cai*
(*Key Laboratory of Mesoscopic Chemistry of Ministry of Education, School of Chemistry and Chemical Engineering, Nanjing University, Nanjing* 210093)

Abstract: Single-phase $Na_2Ti_3O_7$ nanobelts with a width of 20~240 nm, a thickness of 10~40 nm, and a length up to tens of micrometers were synthesized by a two-step hydrothermal reaction of butyl titanate with a concentrated NaOH solution. The structures and morphologies of the nanobelts were characterized by X-ray diffraction and transmission electron microscopy, respectively. Then the nanobelts were fabricated into a chemiresistive sensor for its gas-sensing properties evaluation. The results indicate that the sensor is obviously sensitive to acetone, ethanol, and carbon disulfide at 350~400 ℃ while it is almost insensitive to CO, benzene, NH_3, and 30% formaldehyde solution. The gas-sensing mechanism could be explained by chemisorption model.

Key words: hydrothermal synthesis; titanium; oxides, nanobelts; gas sensors

Oxides become the basis of smart and functional materials due to the fact that the physical and chemical properties of the oxides can be tuned by varying their structure characteristics including valence states of cations, deficiencies of anions, and dimensions, so a considerable attention has been attracted for synthesis and device fabrication of one-dimensional (1D) nanostructures of oxides[1,2]. So far, they have been developed into various functional materials and nanodevices such as Au/CeO_2 nanorod catalysts[3], ZnO nanowire lasers[4], In_2O_3 nanowire field emitters[5], and SnO_2 nanobelt gas sensors[6], and show unique physical and chemical properties. Nanobelts of semiconducting oxide, with a rectangular cross section, are very promising for sensors due to the fact that the surface-to-volume ratio is very high, the oxide is single crystalline, the faces exposed to

收稿日期:2008-02-25。收修改稿日期:2008-07-23。
国家基础研究计划 973(No.2007CB936302)和国家自然科学基金(No.20671050)资助项目。
*通讯联系人。E-mail:wuxingca@nju.edu.cn
第一作者:陶友荣,女,44 岁,副教授;研究方向:纳米材料制备与性能。

the gaseous environment are always the same and the size is likely to produce a complete depletion of carriers inside the belt[6]. Therefore investigation into gas sensor based on nanobelts (nanowires) of semiconducting oxides becomes an important research field[7~11].

Alkali metal titanates ($A_2Ti_nO_{2n+1}$, A=Na, K, Li) usually are composed of negatively charged layered sheets constructed with corner and edge shared TiO_6 octahedra, and alkali metal ions in the interlayers of the titanates[12]. Depending on the alkali metal content they assume various structures (layered or cage structures) and exhibit different properties. For example, sodium trititanate ($Na_2Ti_3O_7$) is crystallized into a monoclinic structure that consists of $Ti_3O_7^{2-}$ layers held together with exchangeable Na^+, while sodium hexatitanate ($Na_2Ti_6O_{13}$) presents a tunnel structure and a good chemical stability. Sodium tri- and hexa- titanates are usual alkali metal titanates, and have widely been applied to plastic reinforcement, photocatalysis, potentiometric gas sensors for O_2 or CO_2[13,14]. The bulk materials can be prepared by solid-state reactions from TiO_2 and Na_2CO_3 or Na_2O at about 1 000 ℃, hydrothermal reactions of TiO_2 powders with NaOH solution, or the sol-gel method from alkoxide precursors[15]. Over the past years, scientists have paid their attention to the synthesis and application of alkali metal titanate nanowires. For instance, Meng and Seo et al. synthesized $Na_2Ti_6O_{13}$ nanowires by hydrothermal reaction of TiO_2 nanoparticles with 10 mol·L^{-1} NaOH solution at 180 ℃ for 12 d[16], and at 250 ℃ for 4 h[17], respectively. Štengl et al. prepared $Na_2Ti_6O_{13}$ nanorods by pyrolysis of sodium titanate glycolate complex, and reported its good photocatalytical activity for the decomposition of 4-chlorophenol[18]. Recently, Kolenko et al. synthesized $Na_2Ti_3O_7$ nanowires by a one-step hydrothermal reaction of amorphous $TiO_2 \cdot nH_2O$ with concentrated NaOH solution, however, they only obtained a mixture of three sodium titanates ($Na_2Ti_nO_{2n+1}$, n=3, 4, 9)[19]. Here we report the preparation of single-phase $Na_2Ti_3O_7$ nanobelts by a two-step hydrothermal reaction, and evaluation of the gas-sensing properties for chemiresistive gas sensor fabricated from the above single-phase $Na_2Ti_3O_7$ nanobelts.

1 Experimental

All chemicals(analytical grade) were purchased from Shanghai Reagents Company and used without further purification. In a typical two-step process, a 3 mL of butyl titanate was added to a 35 mL of 10 mol·L^{-1} NaOH solution, and stirred for 2 min, and then transferred into a 50 mL of Teflon-lined stainless steel autoclave. The autoclave was sealed and maintained at 180 ℃ for 24 h, and then cooled to room temperature. After the autoclave was opened, the suspension was stirred for 2 min again. The autoclave was again sealed and maintained at 180 ℃ for 24 h, and then cooled to room temperature. The final products were filtered and washed with deionized water till pH=7, and then dried at 180 ℃ in air for 6 h.

The obtained products were characterized on a Philips X′ pert X-ray powder diffractiometer (XRD) with Cu $K\alpha$ radiation(λ=0.154 18 nm). X-ray intensities were recorded by X celerator detection system. The size and morphology of the products were determined by a JEOL-JEM 200CX transmission electron microscope (TEM) operating at 200 kV. The chemical composition of the samples was measured by an INCA Energy spectrometer for energy-dispersive X-ray spectroscopy (EDS) attached to a LEO-1530VP field-emission scanning electron microscope (SEM), operating at 20 kV.

The gas sensor was fabricated as follows: a mixture of $Na_2Ti_3O_7$ nanobelts with deionized water was coated onto the Al_2O_3 tube on which two gold electrodes had been installed at each end, and dried slowly in air, and then calcined at 600 ℃ for 2 h in air. The thickness of the nanobelt film was about 200 nm. The Al_2O_3 tube was about 8 mm(l)×2 mm (e.d)×1.6 mm(i.d.). A Ni-Cr wire heater was inserted into the Al_2O_3 tube to supply the operating temperature that could be controlled in the range of 90~500 ℃. The structure of the chemiresistive gas sensor was described in Ref[7].

2 Results and discussion

2.1 Structure and morphology

The powder XRD pattern for the as-prepared sam-

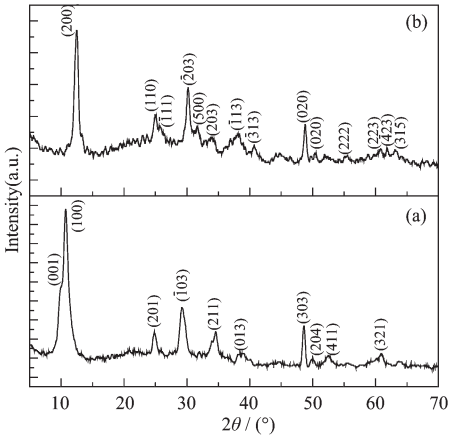

Fig.1 XRD patterns of sodium titanate nanobelts: (a) as-prepared sample; (b) the sample calcined at 600 ℃ for 2 h in air

ple is presented in Fig.1a, which can be completely indexed to monoclinic $Na_2Ti_3O_7$(S.G. $P2_1/m$(11); PDF No. 72-0148) on the base of the peaks position though some peak intensity is different from standard diffraction card. After the $Na_2Ti_3O_7$ nanobelts were calcined at 600 ℃ for 2 h in air, they were converted into another monoclinic phase($Na_2Ti_6O_{13}$)with cell parameters of a= 1.464 nm, b=3.715 nm, c=9.159 nm, and β=99.3°(Fig. 1b). Kolenko et al. once reported that $Na_2Ti_3O_7$ nanowires could be converted into $Na_2Ti_6O_{13}$ nanowires at 500 ℃ in the flowing H_2 for 10 h[19]. In fact, no valence changes in the reaction, so flowing H_2 is not a must in this case. Our results show that the $Na_2Ti_3O_7$ could also be changed to the $Na_2Ti_6O_{13}$ at 500~600 ℃ for 2 h in air, but the cell parameters are slightly less than those of the reported $Na_2Ti_6O_{13}$ (PDF no.73-1398, S.G. C2/m (12), a=1.513 nm, b=3.745 nm, c=9.159 nm, and β=99.3°).

Fig.2a reveals that the as-prepared sample is a nanobelt with a width of 10~230 nm and a length up to several tens of micrometers. A typical nanobelt has a rectangular cross-section with about 20×40 nm^2, shown as white arrow in Fig.2b. SAED (selected area electron diffraction) of a single nanobelt (inset in Fig.2c) indicates that the nanobelt is single-crystalline, and can be indexed to monoclinic $Na_2Ti_3O_7$ PDF no.72-0148), and grows along to [101] direction. In addition, the EDS spectrum of a single nanobelt shows that the average contents of titanium and sodium are 8.80 and 14.76 atom% (Ti/Na ratio 1.68) (Fig.2d). After the $Na_2Ti_3O_7$ nanobelts were fabricated to gas sensor and annealed at 600 ℃ for 2 h in air, they still were single-crystalline nanobelts(Fig.2e and f), but the $Na_2Ti_3O_7$ nanobelts were converted into the $Na_2Ti_6O_{13}$ nanobelts, whose XRD pattern was shown in Fig.1b. So the real sensing materials are the $Na_2Ti_6O_{13}$ nanobelts.

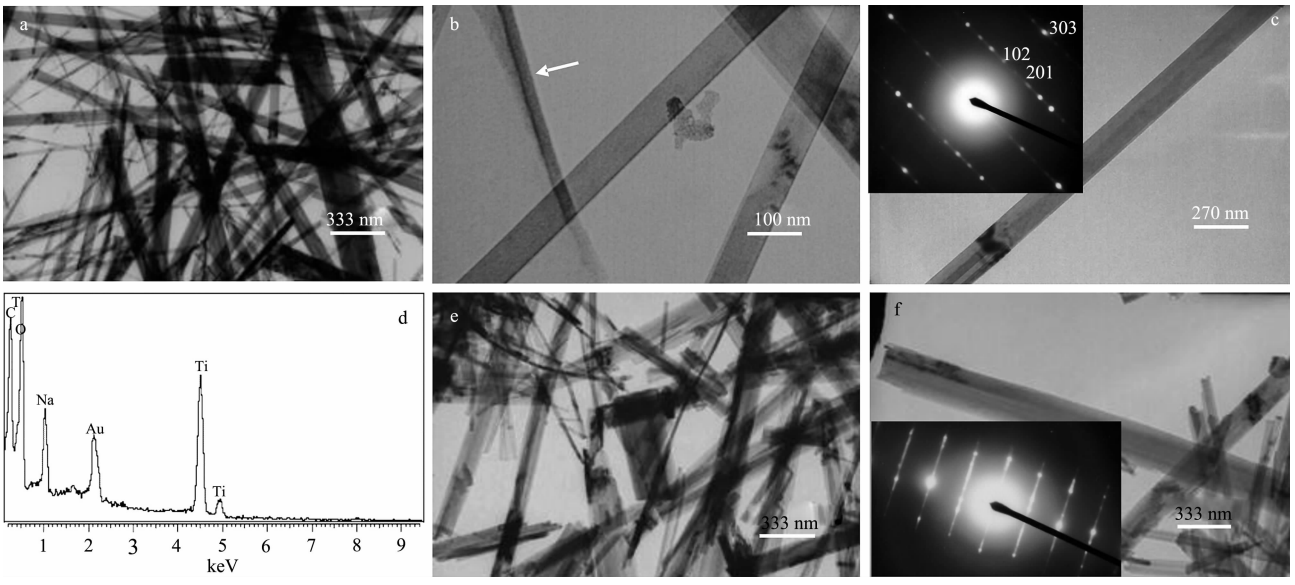

Fig.2 TEM images and EDS spectrum of the $Na_2Ti_3O_7$ nanobelts: (a) overview; (b) magnified micrograph; (c) TEM image and SAED pattern of a single nanobelt; (d) EDS spectrum of a single nanobelt. (e) TEM image after the sample calcined at 600 ℃ for 2h; (f) TEM image and SAED pattern of a single nanobelt of the sample calcined at 600 ℃ for 2 h

2.2 Gas sensing properties

Gas-sensing measurements were made in a static system and the test gas was introduced into the testing chamber by injection. The circuitry of the gas-sensitivity measurement was depicted in Ref. 20. The sensitivity of the sensor(S) was defined as $S=R_a/R_g$, where R_a and R_g are the resistance of the sensor in atmospheric air and in sample-air mixed gas, respectively. In the experiment, a load resistor(R_L) is 300 MΩ, and a circuit voltage(V_C) is 1.56 V. The purity of the measured chemicals including acetone, ethanol, carbon disulfide and benzene is more than 99.5 wt.%. The purity of NH_3 gas is 99 mol.%. CO species comes from a mixture of CO(10 mol.%) and He(90 mol.%), and NO_x species from a mixture of NO (8 mol.%) and He(92 mol.%).

Fig.3 displays the dependence of the resistance of the sensor in air on the operating temperature, revealing that the resistance decreases with the temperature increasing. Fig.4 shows the dependence of the sensitivity of 200 μL·L^{-1} CS_2, ethanol and acetone in ambient air on the operating temperature, which indicates that the as-prepared gas sensor is sensitive to acetone, ethanol and CS_2 in the working temperature, so optimal working temperature is 375 ℃.

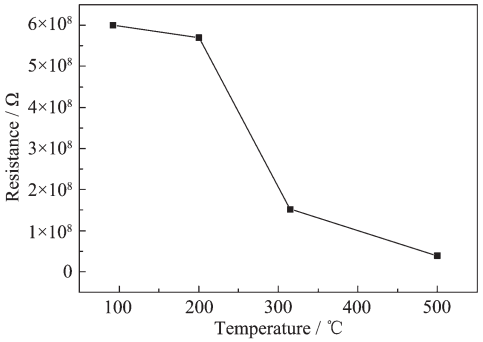

Fig.3　Dependence of the resistance of the sensor in air on the operating temperature

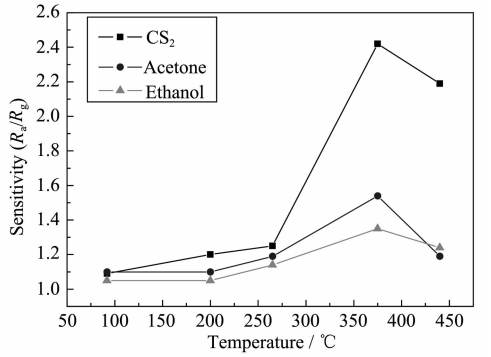

Fig.4　Dependence of the sensitivity of 200 μL·L^{-1} CS_2, ethanol and acetone in ambient air on the operating temperature

Because the sensitivity at 350 ℃ reaches 90% of maximum, the temperature may be selected as a work temperature. Fig.5 displays typical isothermal response curves of acetone, ethanol and carbon disulfide when cycled through increasing the gas concentration in the range of 20~2 000 μL·L^{-1} and ambient air at 350 ℃. It shows that the sensor is sensitive to acetone, ethanol and CS_2, and the highest sensitivity to CS_2. In addition, the sensor has the rapid response/recovery properties. Table 1 shows the response and recovery time of 200 μL·L^{-1} acetone, ethanol and carbon disulfide, with the response time defined as the time required for

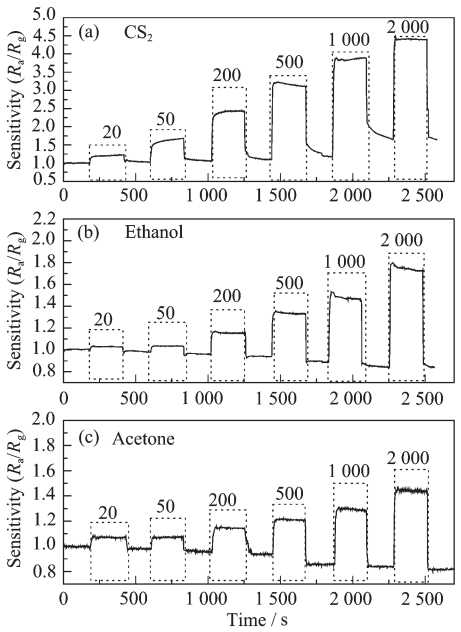

Fig.5　Typical response curves on cycling between increasing concentration(20~2 000 μL·L^{-1}) of gases and ambient air at 60% RH(relative humidity at 20 ℃) on the operating temperature of 350 ℃. (a) CS_2; (b) ethanol; (c) acetone

Table 1　Response/Recovery time of 200 μL·L^{-1} gases at 350 ℃

Gases	Sensor signal (R_a/R_g)	Response time / s	Recovery time / s
CS_2	2.4	13	23
Ethanol	1.2	6	6
Acetone	1.2	8	29

the sample sensitivity variation to reach 90% of the equilibrium value following an injection of test gas and the recovery time defined as the time necessary for the sample to return to 90% the original resistance in air after the test gas has been released.

With regard to practical use, the selectivity of the sensor is measured to other gases. The sensor is almost insensitive to CO, benzene, NH_3, 30% formaldehyde solution at 350 ℃, while it is low sensitive to NO_x. The influence on the response amplitude of the relative humidity (RH) of the environment has been studied. The responses of the sensor in different RH(40%~70%) are almost unchangeable, so the sensor can be applied in wide range of the humidity.

For n-type semiconductor oxide sensors, an acceptable gas-sensing mechanism is surface conduction modulation based on the chemisorption [20,21]. Because $Na_2Ti_6O_{13}$ is an n-type semiconductor, the sensor should follow to the above sensing mechanism. As shown in Fig.6(a), oxygen and water molecules from the ambient air are adsorbed on the surface of $Na_2Ti_6O_{13}$ nanobelts,

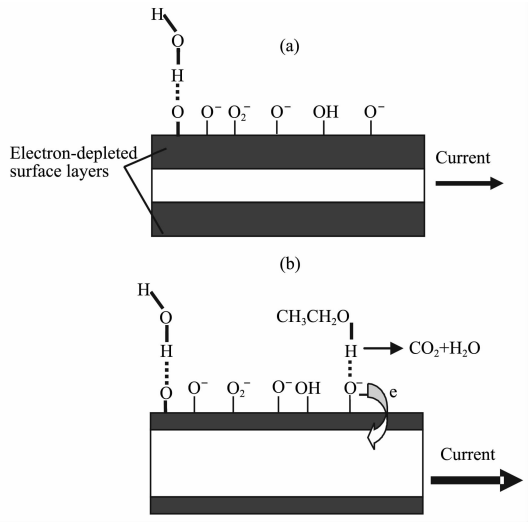

Fig.6 (a) Schematic representation of the mechanism of reaction of $Na_2Ti_6O_{13}$ nanobelt sensor to ethanol. In air, negatively charged oxygen adsorbates(O^-, O_2^-) cover the surface of the belt and results in electron depleted surface layer due to electron transfer from the belt surface to the adsorbates; (b) In ethanol gas, oxygen adsorbates react with the adsorbed ethanol molecules attached by hydrogen bonds, release the trapped electrons, and cause the current to increase

and extract electrons from the $Na_2Ti_6O_{13}$ conduction band so that oxygen is converted into O^- and O_2^- while water into hydroxyl group. Here the concentration of O^- is believed to be dominant. Consequently, the depletion layers are formed in the surface and the grain-boundary regions of the nanobelt, causing the carrier concentration to decrease.

When the sensor is exposed to reducing gases such as ethanol, the ethanol will react with the adsorbed O_{ads}^-, i. e. $CH_3CH_2OH + 6O_{ads}^- \rightarrow 2CO_2 + 3H_2O + 6e$ [20], releasing the trapped electron back to the conduction band, so that the carrier concentration of the nanobelts increases, and the conductivity rises, as shown in Fig.6 (b). Similarly, when sensor is exposed to acetone and CS_2 gases, the adsorbed O_{ads}^- reacts with these gases, respectively, releasing the trapped electron back to the conduction band, so that the carrier concentration of the nanobelts increases, and the conductivity rises. Considering that the reactions are redox process, we conjecture the reaction equations as follows:

$$CH_3COCH_3 + 8O_{ads}^- \rightarrow 3CO_2 + 3H_2O + 8e \quad (1)$$

$$CS_2 + 6O_{ads}^- \rightarrow CO_2 + 2SO_2 + 6e \quad (2)$$

3 Conclusions

A large number of single-phase $Na_2Ti_3O_7$ nanobelts have been synthesized by a two-step hydrothermal reaction. A chemiresistive gas sensor based on the $Na_2Ti_3O_7$ nanobelts has been developed, and shows sensitivity to acetone, ethanol, and carbon disulfide. In addition, research result still shows that $Na_2Ti_3O_7$ can be converted into $Na_2Ti_6O_{13}$ above 500 ℃ in air.

References:

[1] Dai Z R, Pan Z W, Wang Z L. *Adv. Funct. Mater.*, **2003**,**13**: 9~24

[2] Wu X C, Hong J M, Han Z J, et al. *Chem. Phys. Lett.*, **2003**, **373**:28~32

[3] Huang P X, Wu F, Zhu B L, et al. *J. Phys. Chem. B*, **2005**,**109**: 19169~19174

[4] Huang M H, Mao S, Feick H, et al. *Science*, **2001**,**292**:1897~1899

[5] Li S Q, Liang Y X, Wang T H. *Appl. Phys. Lett.*, **2005**,**87**: 143104~143106

[6] Comini E, Faglia G, Sberveglieri G, et al. *Appl. Phys. Lett.*, **2002**,**81**:1869~1871

[7] Chu X F, Wang C H, Jiang D L, et al. *Chem. Phys. Lett.*, **2004**, **399**:461~464

[8] Chen Y J, Nie L, Xue X Y, et al. *Appl. Phys. Lett.*, **2006**,**88**: 83105~83107

[9] Polleux J, Gurlo A, Barsan N, et al. *Angew. Chem. Int. Ed.*, **2006**,**45**:261~265

[10]Qian L H, Wang K, Li Y, et al. *Mater. Chem. Phys.*, **2006**, **100**:82~84

[11]Si S F, Li C H, Wang X, et al. *Sens. Actuators B*, **2006**;**119**:52 ~56

[12]Papp S, Kõrösi L, Meynen V, et al. *J. Solid State Chem.*, **2005**, **178**:1614~1619

[13]Ramírez-Salgado J, Fabry P. *Sens. Actuators B*, **2002**,**82**: 34~39

[14]Holzinger M, Maier J, Sitte W. *Sold State Ionics*, **1996**,**86~88**: 1055~1062

[15]Sauvet A L, Baliteau S, Lopez C, et al. *J. Solid State Chem.*, **2004**,**177**:4508~4515

[16]Meng X D, Wang D Z, Liu J H, et al. *Mater. Res. Bull.*, **2004**, **39**:2163~2170

[17]Seo D S, Kim H, Lee J K. *J. Cryst. Growth*, **2005**,**275**:e2371-e2376

[18]Štengl V, Bakardjieva S, Šubrt J, et al. *Appl .Catal. B*, **2006**, **63**:20~30

[19]Kolenko Y V, Kovnir K A, Gavrilov A I, et al. J. Phys. Chem. B, **2006**,**110**:4030~4038

[20]Gao T, Wang T H. *Appl. Phys. A*, **2005**,**80**:1451~1454

[21]Liu J F, Wang X, Peng Q, et al. *Adv. Mater.*, **2005**,**17**:764~767